PCCP

PAPER

View Article Online
View Journal | View Issue

Cite this: *Phys. Chem. Chem. Phys.*, 2023, **25**, 3806

Synchrotron radiation photoemission spectroscopy of the oxygen modified $CrCl_3$ surface†

S. Kazim,[a] D. Mastrippolito,[b] P. Moras,[c] M. Jugovac,[c] T. Klimczuk,[d] M. Ali,[be] L. Ottaviano[bf] and R. Gunnella *[ag]

Received 1st October 2022,
Accepted 17th December 2022

DOI: 10.1039/d2cp04586a

rsc.li/pccp

We investigate the experimentally challenging $CrCl_3$ surface by photon energy dependent photoemission (PE). The core and valence electrons after cleavage of a single crystal, either in a ultra-high vacuum (UHV) or in air, are studied by keeping the samples at 150 °C, aiming at confirming the atomic composition with respect to the expected bulk atomic structure. A common spectroscopic denominator revealed by data is the presence of a stable, but only partially ordered Cl–O–Cr surface. The electronic core levels (Cl 2p, Cr 2p and 3p), the latter ones of cumbersome component determination, allowed us to quantify the electron charge transfer to the Cr atom as a net result of this modification and the increased exchange interaction between metal and ligand atoms. In particular, the analysis of multiplet components by the CMT4XPS code evidenced the charge transfer to be favored, and similarly the reduced crystal field due to the established polarization field. Though it is often claimed that a significant amount of Cl and Cr atomic vacancies has to be included, such a possibility can be excluded on the basis of the sign and the importance of the shift in the binding energy of core level electrons. The present methodological approach can be of great impact to quantify the structure of ordered sub-oxide phases occurring in mono or bi-layer Cr trihalides.

1 Introduction

2D van der Waals solid like Cr-trihalides have attracted considerable attention in recent years.[1,2] In particular, CrI_3 has been studied in detail because of the possible implementation of 2D magnetism for spintronics,[3] the technology that, exploiting the electron spin degree of freedom, has the best expectations for boosting the performances of nowadays electronic circuits. Such iconic applications will be based on the effects related to magnetooptics and magnetoconductivity,[4,5] both engineered by stacking 2D materials, whose resulting properties will be decisive to the integration of ultra-sensors and other quantum technologies. Also, other 2D materials like tellurides and chalcogenides can be used to harness[6] the spin degree of freedom in charge carriers, without the inconvenience of magnetic dopants leading to the segregation of the metallic phase. Furthermore, as materials with an open electronic band, the use of field effect architectures has clear advantages with respect to zero energy band gap materials like graphene.[7] All these advancements are based on the deep understanding of the low dimensionality ferromagnetism as initially demonstrated by Huang and coworkers in the particular case of CrI_3.[2] The entire Cr-trichloride family has greatly attracted the researchers' attention because of low cleavage energy between planes (0.2 J m^{-2}) and high in-plane stiffness and Young's modulus, comparable to that of graphene of about 1 TPa.[8,9] Furthermore, important structure–property relationships have been settled up; those controlled by the type and number of defects, like atomic site vacancies[10] or those as a direct consequence of the proximity effect.[11] All three Cr compounds ($CrCl_3$, $CrBr_3$, CrI_3) exhibit strong intralayer ferromagnetic coupling, but the interlayer coupling affects variously the final magnetic properties. $CrCl_3$ with anti-ferromagnetic coupling has a Néel temperature below 20 K; $CrBr_3$ and CrI_3 have their

[a] *School of Science and Technology Physics Section University of Camerino, Via Madonna delle Carceri 9, 62032 Camerino, MC, Italy. E-mail: roberto.gunnella@unicam.it*
[b] *Dipartimento di Scienze Fisiche e Chimiche (DSFC), Università degli Studi dell'Aquila, Via Vetoio 10, 67100 L'Aquila, Italy*
[c] *Istituto di Struttura della Materia-CNR (ISM-CNR), S.S. 14, Km 163,5, 34149 Trieste, Italy*
[d] *Faculty of Applied Physics and Mathematics, and Advanced Materials Centre, Gdansk University of Technology, ul. Narutowicza 11/12, 80-233 Gdansk, Poland*
[e] *Department of Physics, Division of Science and Technology, University of Education Lahore, Jauharabad Campus, Pakistan*
[f] *CNR-SPIN UoS L' Aquila, Via Vetoio 10, 67100 L'Aquila, Italy*
[g] *INFN-Sez. Perugia, Via Pascoli Perugia, Italy*

† Electronic supplementary information (ESI) available. See DOI: https://doi.org/10.1039/d2cp04586a

ferromagnetic coupling and Curie temperatures at about 40 and 60 K, respectively. Another fact that distinguishes that $CrCl_3$ is the easy plane character with respect to the easy axis magnetism of the heavier halides, due to the different magnetic anisotropy energy (MAE).[12] The possible transition from in-plane to in-axis magnetism is a complicated interplay between spin–orbit coupling, MAE and the crystal field, representing non-trivial information to be retrieved from total energy calculations.[9] In this regard, the study of one of the most air exposure resistant chromium halides,[6] $CrCl_3$ raises some questions about the presence of intrinsic and extrinsic structural modifications (defects, surface passivation, *etc.*[13]) that could be exploited to expand the material properties and its interaction with external fields. The CrX_3 family crystallizes at low temperatures in a rhombohedral $R\hat{3}$ structure (*i.e.*, BiI_3 like) with transition to monoclinic ($C2/m$),[9] with metal ions in a honeycomb coordinated geometry with Cl_6 edge-sharing octahedra. As a result, trilayers of Cl–Cr–Cl are stacked along the *c*-axis (c = 0.69 nm) while the thickness (Cl–Cl distance) is 0.27 nm as sketched in Fig. 1 for the in-plane and vertical sections of the surface structure. In the same sketch, the possible hollow adsorption position of oxygen is shown. The characteristic properties of $CrCl_3$ with respect to other halides might be related to the presence of a native termination layer[14,15] behaving differently from the normal state, resulting in a material with electronic charge transfer (CT) rather than a pure Mott–Hubbard (MH) system[16] with strong implications for the resulting magnetization. The magnetic properties of $CrCl_3$ have been recently reported in ref. 17.

In fact, Cr-trihalides belong to the Mott–Hubbard (MH) insulators family, whose p-states do not contribute to the valence electrons while the d-states are responsible for the transport and magnetic properties. Nevertheless, upon varying the radii of the atomic components, the presence of hybridization might induce 2D materials to increase charge transfer to obtain half-metallicity (HM) *i.e.*, the presence of a metallic spin channel and insulating one in a manner different from the Mott–Hubbard mechanism.[18] Several transition metal compounds are predicted to exhibit such a half-metallic character. There are Density Functional Theory (DFT) studies that predicted the transition from the insulator to HM in trihalides after introducing point defects, chemisorbed atoms and carrier dopants at specific locations affecting in various ways the magnetic properties.[6,19,20] Another important defect type is the atomic vacancy site also proposed as a way to reach half-metallicity.[19] In fact, the above modifications might induce the ferromagnetism (FM) of 2D materials even though their bulk counterparts are antiferromagnetic (AFM).[21] After doping by means of holes/electrons in a two-dimensional Cr–O–Cl hexagonal system, the enhancement of FM interaction by super-exchange coupling between Cr atoms mediated by the anion/halogen atom might occur. Such enhancement is assisted by structural distortion, and consequent filling of the d_{z^2} state from the initial $t_{2g}^{\uparrow}{}^{\uparrow}{}^{\uparrow}$ configuration as expected for Cr^{+3} atoms.[6] In a previous work, we determined the valence electron structure of the same system after exfoliation in air, by means of valence band PE and scanning tunnelling spectroscopy (STS) with the aim to single out the formation of a Cr–Cl–O hybridization state, correctly identified by total energy calculations.[15] The above study established the link to a possible future technological implementation of the material, but a necessary validation under vacuum conditions is one of the aims of the present paper. Experimental attempts to investigate beyond the application-oriented properties must rely on X-ray absorption, emission[22] and photoemission spectroscopy (PES).[23] In particular, the latter is an ineludible way to characterize the surface and modifications occurring during the preparation. Its surface sensitivity achieved by the short-range character of the electrons when passing through the matter at a few tens of eV kinetic energy,[24] is able to better depict the properties of the most superficial layer of the crystal under study. To this aim, the tuning of the photon energy guaranteed by the synchrotron radiation facilities is an enormous advantage.

In the present work, the surface represents our best approximation of 2D crystals with quality comparable to the bulk material.[25] On the other side, optical techniques or electron microscopy techniques are less sensitive as they average over several layers of the sample or include unwanted topographic defects like in STS. Photon energy-dependent PE by using synchrotron radiation is described in Section II. In Section III the analysis of photoemission spectra of electrons from core levels will be described, together with the estimation of the electronic charge transfer between the neighbour atoms. Similarly, the spectra from the valence band and their dependence on the photon energy reinforcing the results are reported as well. Finally, conclusions follow in Section IV.

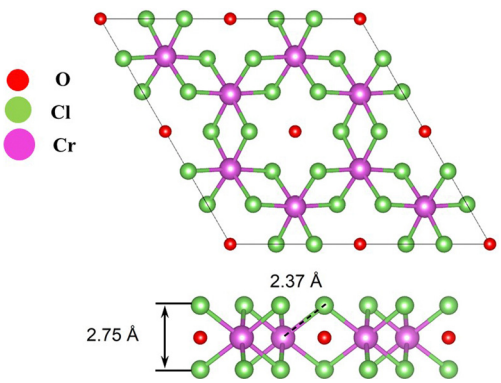

Fig. 1 Atomic arrangement of the O-$CrCl_3$ monolayer structure.

2 Materials and methods

High-quality crystals of $CrCl_3$ were provided by the group of Prof. Tomasz Klimczuk and the preparation was explained in detail in the ESI† and in recent references 26 and 27. Some members of our group have reported the unexpected magnetic properties of exfoliated $CrCl_3$ compared to the bulk, which are also provided in the ESI.†

To expand our knowledge about the system, we performed X-ray photoemission spectroscopy (XPS) measurements using a

tunable and monochromatized photon energy source (0.1 × 0.3 mm) available at the "VUV-Photoemission" beamline of the Elettra synchrotron in Trieste. The photon energy was varied between 40 and 700 eV, with horizontal polarization and with an incidence angle of 45°. The spectra were acquired using a Gammadata Scienta R4000WAL analyzer in a normal emission geometry, with a total energy resolution (light source and electron analyser) of about 0.1 eV, while maintaining the sample temperature at 150 °C in order to prevent charging effects. The binding energy (BE) scale was calibrated by using adventitious carbon as a reference at 284.8 eV. We used Fityk 1.3.1 data analysis software for processing Cl 2p core level data after subtracting the Shirley background while the Voigt line shape was used for multicomponent analysis of the spectra. The Cr core levels could not be treated similarly because of the multiplets taking place of the atomic doublet. With regard to the Cr 2p and 3p analyses a conventional treatment of spectrum components[28] by means of Voigt functions, would lead to unrealistic lineshape parameters (spin–orbit splitting and branching ratios). For the above reason, we took advantage of a multiplet component analysis based on calculations from the CTM4XPS program.[29–31] The procedure for the determination of the transfer of electronic charge has been described in detail in the ESI† and the parameters used for the calculations are listed in the following together with transfer parameters for reference materials $CrCl_3$[16] and Cr_2O_3.[32]

3 Results and discussion

3.1 Survey spectra

In Fig. 2, we present the PE survey spectrum at 150 °C sample temperature with 700 eV and 650 eV photon energies for the samples cleaved *in situ* (Fig. 2(a)) and *ex situ* (Fig. 2(b)), respectively. The effect of oxygen contamination in *ex situ* samples is evident and indicates mainly contributions equivalent to the hydro-oxide origin (O 1s binding energy at 532 eV) at both photon energies, 700 eV and 650 eV. The composition analysis based on the PE intensity ratio of Cl 2p and Cr 2p components gives the expected Cl/Cr stoichiometry value, *i.e.*, 3 : 1.

Weak C 1s and O 1s signals were also visible in the *in situ* cleaved sample. The corrected atomic sensitivity ratio was derived thoroughly in the ESI.† The modification of $CrCl_3$ was studied by improving the surface sensitivity of the PE experiment by changing the photon energy.

To investigate the surface character, we compared the spectra recorded at normal emission at 700 eV photon energy, corresponding approximately to 1 nm probing depth, with those having higher surface sensitivities obtained by lowering the photon energy. The amount of oxygen in *in situ* cleaved samples corresponded to 1% and 2% of the Cl 2p peak at, respectively, 700 and 650 eV. If corrected for the 1 : 2 factor of the atomic sensitivity of O with respect to Cl at about 700 eV photon energy,[33] we can estimate for *in situ* cleaved samples an amount of 1 to 4% in oxygen while going from 700 to 650 eV and correspondingly increasing the sensitivity towards the surface. This amount is about a factor 5–10 times less than that observed in *ex situ* prepared samples and it is of different character as will be evident below.

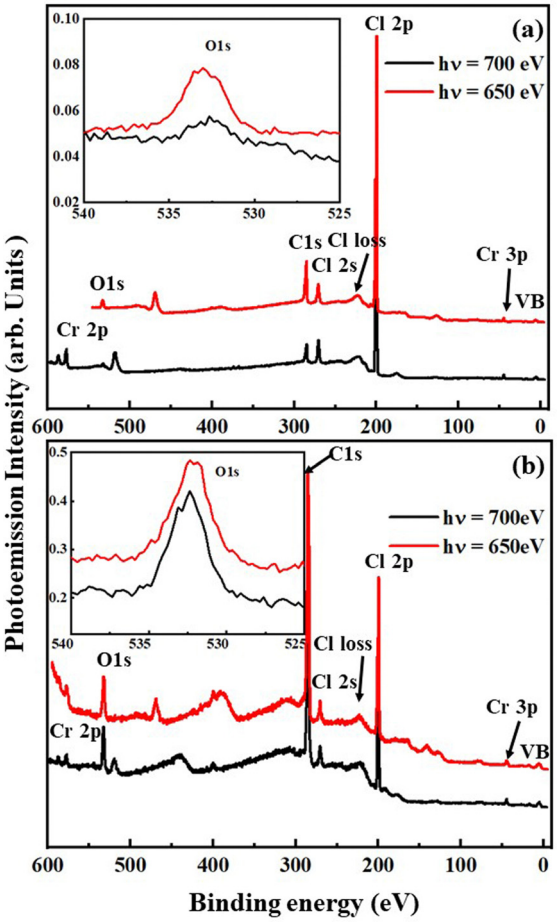

Fig. 2 Survey photoemission spectra normalized at the Cl 2p peak of cleaved $CrCl_3$ at 700 eV and 650 eV photon energies, respectively: (a) in UHV and (b) in air. The insets show the relative O 1s components. Also visible, among other labelled peaks, are the Auger LMM from Cl and KVV Auger from C at 175 and 265 eV kinetic energies.

3.2 Cl 2p core level

Fig. 3 shows the Cl 2p core levels with different photon energies of UHV cleaved (Fig. 3(a)) and air cleaved (Fig. 3(b)) samples. The parameters of the Cl 2p core level fitting are listed in Table 1.

The spin–orbit splitting energy value of Cl 2p doublets is between 1.55 eV and 1.6 eV, and the branching ratio varies around the expected 1 : 2 value by less than 20%. This deviation in the branching ratio may be related to the angular resolution of the analyzer and to photoelectron diffraction effects.[34] Gaussian broadening equal to 2 ln(2) × Gw and full width half maximum (FWHM) were varied by less than 10% during photon energy tuning. The parameters used for the fitting are explicitly listed in Table 1 for each photon energy, including the branching ratios (BRs) and the spin orbit (SO) splitting of the Cl 2p doublet.

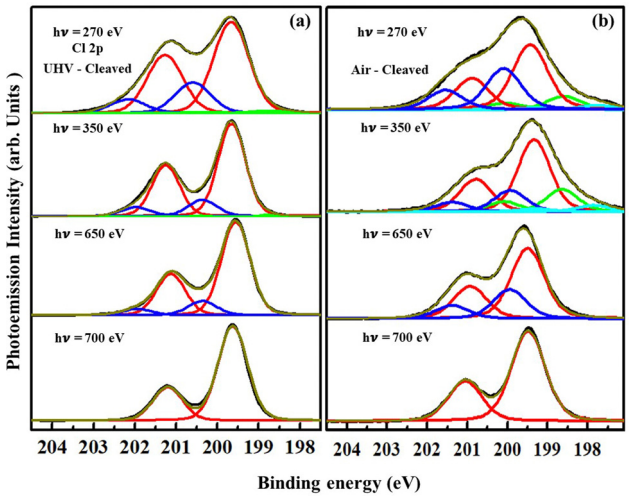

Fig. 3 Normalized Cl 2p PE core level spectra of UHV cleaved (a) and air cleaved (b) $CrCl_3$. Photon energy was varied from 700 to 270 eV to increase surface sensitivity.

Table 1 Parameters used to fit Cl 2p spectra at 150 °C for all photon energies mentioned under both cleaving environmental conditions

Parameters used for Cl 2p fitting for $CrCl_3$					
Exp.	$h\nu$ (eV)	Gw (eV)	FWHM (eV)	SO (eV)	BR
Vacuum	700	0.47	0.85	1.57	0.35
	650	0.46	0.83	1.57	0.45
	350	0.45	0.86	1.6	0.55
	270	0.57	1.0	1.57	0.45
Air	700	0.53	1.0	1.57	0.43
	650	0.54	1.0	1.55	0.46
	350	0.53	1.1	1.57	0.45
	270	0.53	1.1	1.57	0.47

The main component is found at 199.6 eV binding energy. With surface sensitivity, a second peak is seen at a higher binding energy (≈0.9 eV). This fact excludes the case of Cl vacancy sites on the surface of Cr trichloride, already observed at lower binding energies after prolonged annealings at $T \geq 200$ °C.[15] This would rather create the conditions of increased charge available from the Cr first neighbours for each Cl atom, leading to a lower binding energy component of the Cl 2p core level, that we cannot detect within the sensitivity of the technique. After annealing at 300 °C (see the ESI†) clear signatures of vacancy formation are eventually observed. Similarly, the presence of lower energy shift components is evident in the air-cleaved samples of Fig. 3(b). The higher binding energy component of Cl 2p in Fig. 3(a) covers from 0% to 30% of the main peak when changing to more surface sensitive energies (top curves) and at the first sight is of unclear origin. This must be assigned to the formation of a Cr–O–Cl surface phase as the component is not seen in the experiment of Mastrippolito *et al.*[15] done in bulk sensitivity/air cleaved experiments. We stress that the present feature is not due to a simple Cr oxidization and cannot be relegated to the case of adventitious oxidation of the surface. As no interaction occurs between Cl and O, the origin of that shift is related to the energy stability induced by the charge transfer to Cr(III) atoms and of the consequent transition from a Cr low spin state $S = 3/2$ to a high spin $S = 2$ configuration that might be even 2 eV more stable[35,36] than the low spin state. A consequence would be the distortion of the local geometry and relaxation of the Cr–Cl bond leading to a high energy shift of the core level. In particular, the Cl–Cr–Cl bond will assume two different configurations with bond angles different from 90° but split into two of 98° and 83° respectively. In addition a slight extension of the bond length due to oxygen intercalation and consequent interlayer distance expansion also occurred.[15]

3.3 Cr 2p core level

Partial occupation of d states in transition metal compounds gives origin to electronic multiplets in PE spectra.[29] Fig. 4 upper panel, presents the Cr 2p core level spectra taken on the vacuum cleaved sample at 700 eV and 650 eV photon energies with the main peak of $CrCl_3$ observed at 577.3 eV binding energy and with a clear presence of a lower energy (1.2 eV) component increasing in importance with the increase of surface sensitivity at 650 eV photon energy. Such a component could be related to Cr–O–Cl surface formation. The incomplete oxide phase is attested by the missing low binding energy

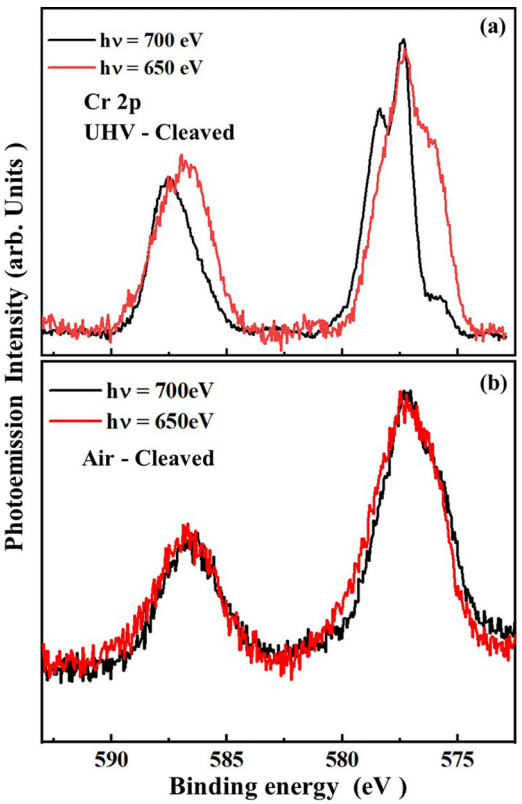

Fig. 4 Cr 2p core level spectra acquired at 700 eV and 650 eV photon energies while samples were kept at 150 °C temperature: (a) normalized spectra of Cr 2p after UHV cleavage; (b) normalized experimental spectra after cleavage in air.

component (below 576 eV)[37] typical of the Cr_2O_3 compound. In the lower panel, the measurements on samples cleaved in the air show, as expected, a minor sensitivity with respect to photon energy. It is also visible that the oxide phase is different from that of the upper panel obtained during UHV preparation, because the components are no more visible, the hint of thick oxide layer formation.

In Fig. 5(a) the spectrum taken at 700 eV, for the samples cleaved in UHV, has been reproduced with components calculated using CTM4XPS with parameters reported in Table 2. The contribution of Cr 2p with two different charge states, namely $CrCl_3$ and the state called CT (charge transfer), in a ratio of 9 : 1 is the best combination which fits the experiment at 700 eV in Fig. 5(a). The individual curves obtained by CTM4XPS were also plotted in Fig. 5(b) for the experiment at 650 eV. In this case, a 4 : 6 ratio is obtained with a predominance of the CT component and slight broadening implying a certain degree of disorder. The main information obtained from the comparison of the calculated Cr 2p spectra is the increase of a CT phase, which we can claim to be related to the presence of a structure as reported in Fig. 1. In the case of full occupation of oxygen in

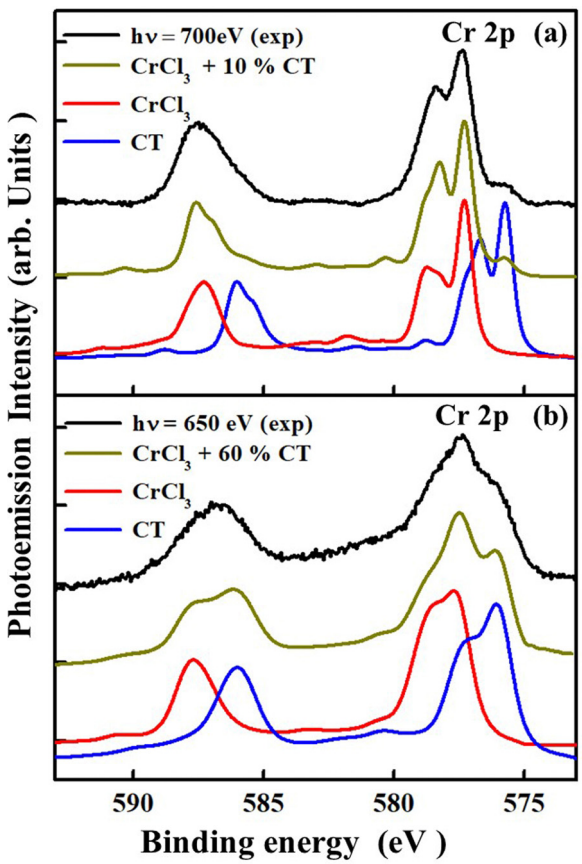

Fig. 5 Comparison of CTM4XPS calculations for experimental Cr 2p core levels at (a) 700 eV and (b) 650 eV photon energy. Experimental curves (black curves) are fitted as a linear combination (yellow curves) in ratios of 9 : 1 and 4 : 6, respectively, for multiplets related to the state $CrCl_3$ and the modified surface one called "CT". Such calculations are also reported before the linear combination (red and blue curves).

Table 2 Parameters used in charge transfer studies for Cr 2p PE core level spectra and the cases of $CrCl_3$ and Cr_2O_3 from the literature.[16,32] The interaction parameters used in the table denote the following: crystal field (10 D_q), the charge transfer energy (Δ), average Coulomb interaction ($U_{dd} - U_{pd}$), 3d–3d coulomb repulsive energy (U_{dd}), and energy splitting (T_e and T_{2g}).[29] Note that the T_{eff} value is about 4 times the splitting energy T_{2g}

CMT4XPS parameters for Cr 2p fitting

Compounds	d^n	Delta	U_{dd}	U_{pd}	10 D_q	T_e	T_{2g}
$CrCl_3$	d^3	5.4	3.3	3.2	2.0	1.6	0.8
CT	d^3	5.5	5.5	6.0	0.5	2.0	1.0
$CrCl_3$[16]	d^3	6.5	3.3	6.0	—	T_{eff} = 3.6	—
Cr_2O_3[32]	d^3	5.5	5.5	6.0	—	T_{eff} = 7.6	—

"hollow" positions, following the model of Mastrippolito *et al.*,[15] the O–$CrCl_3$ surface would have a composition given by Cl : Cr : O equal to 24 : 8 : 3, *i.e.*, the oxygen would be about 9.5% of the atomic composition. Actually, a maximum content of 5% of atomic oxygen was measured from the PE intensity of the O 1s core level in Fig. 2. We can conclude that the coverage of this heterogeneous phase corresponds to about 50% of the surface. Such a value must be intended as a lower limit because of the depth profile sensitivity of the XPS, which is slightly larger than the thickness of the layer structure of about 2.75 Å, as reported in Fig. 1. We calculated in Fig. 6, the 90% confidence interval of the intensity ratio ($CrCl_3$-CT)/$CrCl_3$ of the Cr 2p core level at various electron mean free paths (MFPs) depending on the photon energy. The two values reported in red squares in Fig. 6 correspond to the experimental ratio intensities of surface to the bulk component of 1.5 and 0.12 respectively, as found for photon energies of 650 eV (estimated MFP about 4 Å) and 700 eV (estimated MFP of 8 Å). The intensity ratio of the two Cr 2p components can be calculated using following eqn (1)[38] as a function of the mean free path λ and oxide phase coverage

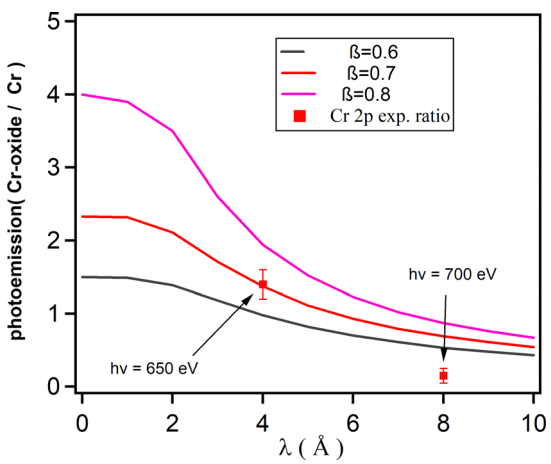

Fig. 6 Intensity ratio of surface vs bulk Cr 2p components taken at 650 and 700 eV, respectively, as a function of the electron mean free path. The upper and lower curves represent the 90% confidence interval for such an intensity ratio. Comparison with the two experimental determinations (red squares on the basis of the estimated mean free path during the respective photon energy Cr 2p photoemission[38]).

percent β (to be determined):

$$\frac{I_{Cr(CT)}}{I_{Cr}} = \frac{\beta}{(1 - e^{-d/\lambda})^{-1} - \beta} \quad (1)$$

where d is the interlayer spacing (6.9 Å).

As can be observed from the confidence interval, the comparison is well verified for the surface-sensitive case in Fig. 6, with an estimated β = 70% CT phase on the first layer; while the calculation overestimates the Cr–O–Cl component in the bulk sensitive experiment. The latter is the probable occurrence of interlayer forward focusing of photoelectrons also known as the lens effect induced by collinear scattering[39] amplifying the bulk signal. The latter considerations are a further evidence of the high quality of van der Waals crystals because collinear effects would be strongly damped in disordered systems.[40]

Such an effect, enhanced using a high-resolution solid angle acceptance analyser, slightly affects the comparison of the PE intensity with the atomic composition because of the anisotropy of the detected intensity. More reliable is the result obtained with surface sensitive photons. As a direct result of this comparison, the 70% contribution of the oxide phase of Fig. 1 would correspond to the amount of 6% of atomic oxygen. This estimated figure is consistent with the other estimate obtained from the O 1s to Cl 2p peaks ratio taken at 650 eV normalized by respective sensitivity factors of O 1s and Cl 2p (1 : 2). Such an evidence further confirm that the present surface is a stable and chemically ordered termination phase of $CrCl_3$, in principle a candidate to harness the functionality of the 2D properties of the $CrCl_3$ layers. Within this hypothesis, the origin of a Cr 2p lower binding energy shifts after the formation of the O–$CrCl_3$ phase might be due to the O^{-2} ions in "hollow" positions polarizing the entire O–Cr–Cl structure (Fig. 1) in a way similar to the onset of an electrostatic cage on Cr atoms, provided a charge transfer mechanism from Cl 3p levels to Cr 3d ones. The additional covalent bonding induced by the oxygen in position "hollow" would be at the origin of the optimal parameter Δ = 5.5 eV, charge transfer energy lower than the 6.5 eV expected in $CrCl_3$.[16]

Another parameter of the model that had to be reduced was the crystal field of 10 D_q value to 0.5 eV from the nominal value of 2.0 eV, which suggested the transition from the Mott–Hubbard insulator to a polarized metal band configuration.[41]

We note that in the case of hypothetical Cr vacancies,[19] the effect on Cr 2p core electron levels would be mediated by Cl atoms, which would induce a higher oxidation state on the nearby Cr atoms, leading to a higher binding energy that is not observed.

3.4 Cr 3p core level

The correlation effects delineated above were supposed to be even more explicit in Cr 3p electron photoemission, due to the lower energy states involved, leading to increased interaction and hybridization between d metal states and halide p states, resulting in a larger core electron energy level shift (about 1.5 eV). While calculating the Cr 3p multiplets, along with the charge transfer value, we have to take into consideration the amount of Slater integral's reduction and spin–orbit coupling parameters.[29]

Here, we used two 10 D_q values, *i.e.*, 4 eV and 2 eV for spectra related to bulk and surface, respectively, to take into consideration the reasons above. Noteworthily, in all presented cases, we always consider equal to zero the valence spin–orbit parameter.[30,31] We have taken the Lorentzian and Gaussian broadening $\sigma \approx 0.35$ eV for surface sensitive spectra and 0.3 eV for the bulk ones. The parameters used to fit the Cr 3p core electron level spectra are reported in Table 3.

Table 3 Parameters used in charge transfer studies for Cr 3p PE core level spectra. The interaction parameters used in the table denote the following: crystal field (10 D_q), the charge transfer energy (Δ), average Coulomb interaction ($U_{dd} - U_{pd}$), 3d–3d coulomb repulsive energy (U_{dd}), and energy splitting (T_e and T_{2g})[29]

Charge transfer energy for Cr 3p core level							
Compounds	d^n	Delta	U_{dd}	U_{pd}	10 D_q	T_e	T_{2g}
$CrCl_3$	d^3	5.4	3.3	3.2	4.0–2.0	1.6	0.8
CT	d^3	5.5	5.5	6.0	0.5	1.6	0.8

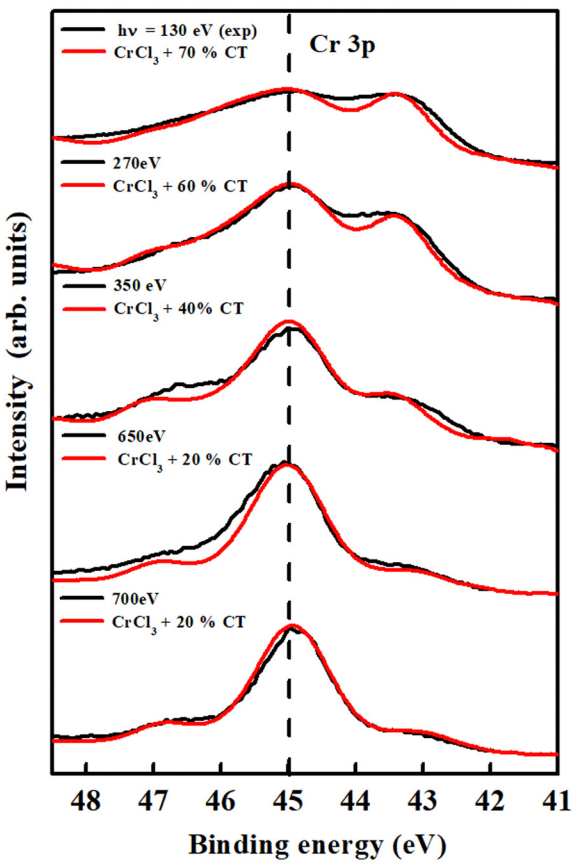

Fig. 7 Cr 3p core level spectra of vacuum cleaved $CrCl_3$: the curves represent the experimental and theoretical spectra of $CrCl_3$ and charge transfer (CT) contributions for the full set of photon energies displaced vertically.

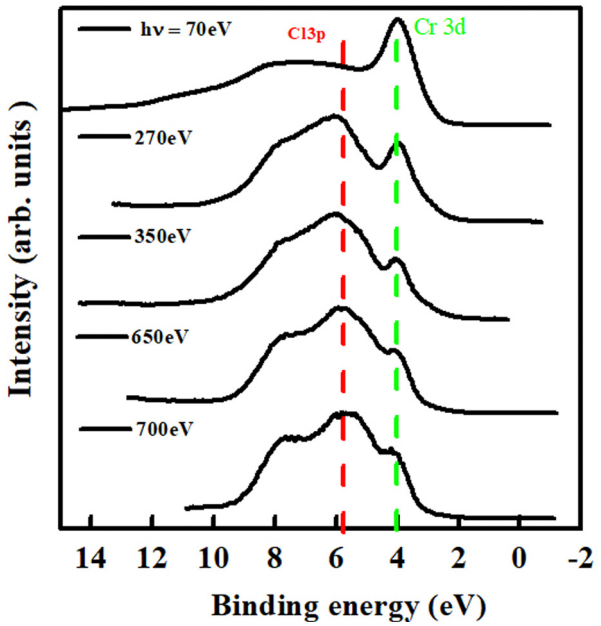

Fig. 8 Valence band spectra of UHV cleaved $CrCl_3$ with the variation of photon energies from 700 to 70 eV. The red and green dotted lines represent the Cl 3p and Cr 3d states.

Fig. 7 shows the Cr 3p spectra where the black curves correspond to the experimental spectra at different photon energies and the red curves are associated with a mix of normal and CT phases. It is quite evident that the CT phase, we supposed due to the O–Cr–Cl contribution, increases from 20% to 70% as one moves to the more superficial layers of the sample by reducing the photon energy.

3.5 Valence states

To study the modification of the electronic character of the p–d hybridization, the valence band spectra were recorded while varying the photon energies from 700 eV to 70 eV. The VB spectra of UHV cleaved $CrCl_3$ are presented in Fig. 8. The positions of Cr 3d and Cl 3p appear at about 4.0 and 5.7 eV binding energy, respectively, while moving towards more surface-sensitive photon energies the Cl 3p state is strongly reduced.[42] The Cl 3p intensity suppression and an increment in the Cr 3d valence state are justified by charge transfer but reflect also the cross-section ratio at different photon energies.[33] Contrarily to what was reported in previous HeI (21.2 eV) valence band PE data, we did not observe any characteristic state at the Fermi edge, probably because of the factor 5–10 lower PE cross-section[33] of such a state at the 70 eV photon energy of the present experiment. An additional effect is the limited annealing temperature, hindering the detection of a long-range ordered surface state.

4 Conclusions

The present work reports on the charge transfer effects mediated by oxygen in chromium tri-chloride during Cl–Cr hybridization. Despite the difficulties in applying electron spectroscopy to the $CrCl_3$ surface, due to the relevant charging, core levels PE spectra appropriately measured allowed the identification of a stoichiometric and ordered oxygen-related phase. Such a phase, amounting to 4–6 atomic percent of oxygen and therefore covering up to 60% of surface hollow sites, is situated between the Cl layers, at the level of the Cr atom layer. In those positions, they are responsible for a net charge transfer to chromium atoms that have been quantified by the present study. Furthermore it results that the characteristics of the core level electron spectra cannot support the evidence of Cl or Cr vacancies, confirming a previous study with the sample preparation under ambient conditions and characterized by complementary experimental techniques, like XPS and TEM.[15] The specificity of the material studied, *i.e.*, the most ambient resistant among Cr tri-halides, suggests that fine dosing of oxygen paves the way for tuning new robust phases of the 2D-magnetic character in such materials deserving dedicated experimental preparations. The present study shows one of the many cases, where the PE analysis of TM ions, in terms of spin–orbit split components of superposed valency states, must evolve towards an approach where surface and bulk components could be represented as originating from different chemical and electronic configurations. In these cases coupling of internal degrees of freedom of TM ions, namely spin and angular momentum, cannot be treated on the same basis for a comprehensive interpretation of the results.

Author contributions

S. Kazim: methodology, data curation, and writing – original draft preparation; D. Mastrippolito: reviewing and methodology; P. Moras: methodology, editing, and reviewing; M. Jugovac methodology; T. Klimczuk: methodology; M. Ali: reviewing; L. Ottaviano: conceptualization; R. Gunnella: conceptualization, methodology, supervision, editing, and reviewing.

Conflicts of interest

There are no conflicts to declare.

Acknowledgements

R. G. received support from Istituto Nazionale di Fisica Nucleare (INFN) within the CSN5 grant QUANTEP. P. M. and M. J. acknowledge funding from the project EUROFEL – ROADMAP ESFRI. TK acknowledges support from the National Science Centre (Poland) within grant UMO-2018/30/M/ST5/00773.

Notes and references

1 C. Gong, L. Li, Z. Li, H. Ji, A. Stern, Y. Xia, T. Cao, W. Bao, C. Wang and Y. Wang, *et al.*, Discovery of intrinsic ferromagnetism in two-dimensional van der Waals crystals,

Nature, 2017, **546**(7657), 265–269, DOI: 10.1038/nature22060.

2 B. Huang, G. Clark, E. Navarro-Moratalla, D. R. Klein, R. Cheng, K. L. Seyler, D. Zhong, E. Schmidgall, M. A. McGuire and D. H. Cobden, *et al.*, Layer-dependent ferromagnetism in a van der Waals crystal down to the monolayer limit, *Nature*, 2017, **546**(7657), 270–273, DOI: 10.1038/nature22391.

3 A. Soumyanarayanan, N. Reyren, A. Fert and C. Panagopoulos, Emergent phenomena induced by spin-orbit coupling at surfaces and interfaces, *Nature*, 2016, **539**(7630), 509–517, DOI: 10.1038/nature19820.

4 Y. Deng, Y. Yu, Y. Song, J. Zhang, N. Z. Wang, Z. Sun, Y. Yi, Y. Z. Wu, S. Wu and J. Zhu, *et al.*, Gate-tunable room-temperature ferromagnetism in two-dimensional Fe_3GeTe_2, *Nature*, 2018, **563**(7729), 94–99, DOI: 10.1038/s41586-018-0626-9.

5 T. Song, X. Cai, M. W.-Y. Tu, X. Zhang, B. Huang, N. P. Wilson, K. L. Seyler, L. Zhu, T. Taniguchi and K. Watanabe, *et al.*, Giant tunneling magnetoresistance in spin-filter van der Waals heterostructures, *Science*, 2018, **360**(6394), 1214–1218, DOI: 10.1126/science.aar4851.

6 Q.-Y. Rong, A.-M. Hu, X.-H. Zhang, L.-L. Wang and W.-Z. Xiao, Ferromagnetism and controllable half-metallicity of two-dimensional hexagonal CrOX (X = F, Cl, Br) monolayers, *J. Magn. Magn. Mater.*, 2020, **515**, 167310, DOI: 10.1016/j.jmmm.2020.167310.

7 S. Wei, X. Tang, X. Liao, Y. Ge, H. Jin, W. Chen, H. Zhang and Y. Wei, Recent progress of spintronics based on emerging 2D materials: CrI_3 and Xenes, *Mater. Res. Express*, 2019, **6**(12), 122004, DOI: 10.1088/2053-1591/ab5d45.

8 J. Liu, Q. Sun, Y. Kawazoe and P. Jena, Exfoliating biocompatible ferromagnetic Cr-trihalide monolayers, *Phys. Chem. Chem. Phys.*, 2016, **18**(13), 8777–8784, DOI: 10.1039/C5CP04835D.

9 W.-B. Zhang, Q. Qu, P. Zhu and C.-H. Lam, Robust intrinsic ferromagnetism and half semiconductivity in stable two-dimensional single-layer chromium trihalides, *J. Mater. Chem. C*, 2015, **3**(48), 12457–12468, DOI: 10.1039/C5TC02840J.

10 B. Shabbir, M. Nadeem, Z. Dai, M. S. Fuhrer, Q.-K. Xue, X. Wang and Q. Bao, Long range intrinsic ferromagnetism in two dimensional materials and dissipationless future technologies, *Appl. Phys. Rev.*, 2018, **5**(4), 041105, DOI: 10.1063/1.5040694.

11 A. Avsar, J. Y. Tan, T. Taychatanapat, J. Balakrishnan, G. Koon, Y. Yeo, J. Lahiri, A. Carvalho, A. Rodin and E. OFarrell, *et al.*, Spin-orbit proximity effect in graphene, *Nat. Commun.*, 2014, **5**(1), 1–6, DOI: 10.1038/ncomms5875.

12 M. A. McGuire, H. Dixit, V. R. Cooper and B. C. Sales, Coupling of crystal structure and magnetism in the layered, ferromagnetic insulator CrI_3, *Chem. Mater.*, 2015, **27**(2), 612–620, DOI: 10.1021/cm504242t.

13 D. Rhodes, S. H. Chae, R. Ribeiro-Palau and J. Hone, Disorder in van der Waals heterostructures of 2D materials, *Nat. Mater.*, 2019, **18**(6), 541–549, DOI: 10.1038/s41563-019-0366-8.

14 B. Sainbileg, E. Batsaikhan and M. Hayashi, Impact of oxygen defects on ferromegnatic CrI_3 monolayer, *RSC Adv.*, 2020, **10**, 42493, DOI: 10.1039/d0ra08153a.

15 D. Mastrippolito, L. Ottaviano, J. Wang, J. Yang, F. Gao, M. Ali, G. D'Olimpio, A. Politano, S. Palleschi and S. Kazim, *et al.*, Emerging oxidized and defective phases in low-dimensional $CrCl_3$, *Nanoscale Adv.*, 2021, **3**(16), 4756–4766, DOI: 10.1039/D1NA00401H.

16 I. Pollini, Charge Transfer Satellites in X-Ray Photoelectron Spectra of Cr Trihalides, *Phys. Status Solidi B*, 2000, **222**(2), 483–493, DOI: 10.1002/1521-3951(200011)222:2<483::AID-PSSB483>3.0.CO;2-H.

17 M. Serri, G. Cucinotta, L. Poggini, G. Serrano, P. Sainctavit, J. Strychalska-Nowak, A. Politano, F. Bonaccorso, A. Caneschi, R. J. Cava, R. Sessoli, L. Ottaviano, T. Klimczuk, V. Pellegrini and M. Mannini, Enhancement of the Magnetic Coupling in Exfoliated $CrCl_3$ Crystals Observed by Low-Temperature Magnetic Force Microscopy and X-ray Magnetic Circular Dichroism, *Adv. Mater.*, 2020, **32**(24), 2000566, DOI: 10.1002/adma.202000566.

18 I. Pollini, Electron Correlation and Hybridization in chromium compounds, *Solid State Commun.*, 1998, **106**, 549.

19 Y. Gao, J. Wang, Y. Li, M. Xia, Z. Li and F. Gao, Point-Defect-Induced Half Metal in $CrCl_3$ Monolayer, *Phys. Status Solidi RRL*, 2018, **12**(7), 1800105, DOI: 10.1002/pssr.201800105.

20 J. Yang, J. Wang, Q. Liu, R. Xu, Y. Sun, Z. Li, F. Gao and M. Xia, Band engineering in intrinsically magnetic $CrBr_3$ monolayer, *J. Magn. Magn. Mater.*, 2020, **502**, 166608, DOI: 10.1016/j.jmmm.2020.166608.

21 B. Miao, N. Xu, L. Zhu, J. Zhou and Z. Sun, 2D intrinsic ferromagnets from van der Waals antiferromagnets, *J. Am. Chem. Soc.*, 2018, **140**, 2417–2420, DOI: 10.1111/jmi.13015.

22 P. Olalde-Velasco, J. Jiménez-Mier, J. Denlinger, Z. Hussain and W. Yang, Direct probe of Mott-Hubbard to charge-transfer insulator transition and electronic structure evolution in transition-metal systems, *Phys. Rev. B*, 2011, **83**(24), 241102, DOI: 10.1103/PhysRevB.83.241102.

23 M. Yan, Y. Jin, Z. Wu, A. Tsaturyan, A. Makarova, D. Smirnov, E. Voloshina and Y. Dedkov, Correlations in the Electronic Structure of van der Waals $NiPS_3$ Crystals: An X-ray Absorption and Resonant Photoelectron Spectroscopy Study, *J. Phys. Chem. Lett.*, 2021, **12**(9), 2400–2405, DOI: 10.1021/acs.jpclett.1c00394.

24 M. De Crescenzi, R. Gunnella, R. Bernardini, M. De Marco and I. Davoli, Auger-electron diffraction in the low kinetic-energy range: The Si (111) 7× 7 surface reconstruction and Ge/Si interface formation, *Phys. Rev. B*, 1995, **52**(3), 1806, DOI: 10.1103/PhysRevB.52.1806.

25 M. Groenke, B. Buschbeck, P. Schmidt, M. Valldor, S. Oswald, Q. Hao, A. Lubk, D. Wolf, U. Steiner, B. Buechner and S. Hampel, Chromium Trihalides CrX_3 (X = Cl, Br, I): Direct Deposition of Micro- and Nanosheets on Substrates by Chemical Vapor Transport, *Adv. Mater. Interfaces*, 2019, **6**(24), 1901410, DOI: 10.1002/admi.201901410.

26 S. Kazim, M. Ali, S. Palleschi, G. D'Olimpio, D. Mastrippolito, A. Politano, R. Gunnella, A. Di Cicco,

M. Renzelli, G. Moccia, O. A. Cacioppo, R. Alfonsetti, J. Strychalska-Nowak, T. Klimczuk, R. J. Cava and L. Ottaviano, Mechanical exfoliation and layer number identification of single crystal monoclinic $CrCl_3$, *Nanotechnology*, 2020, **31**, 395706, DOI: **10.1088/1361-6528/ab7de6**.

27 S. Kazim, R. Gunnella, M. Zannotti, R. Giovannetti, T. Klimczuk and L. Ottaviano, Determination of the refractive index and wavelength-dependent optical properties of few-layer $CrCl_3$ within the Fresnel formalism, *J. Microsc.*, 2021, **283**, 145, DOI: **10.1111/jmi.13015**.

28 M. C. Biesinger, B. P. Payne, A. P. Grosvenor, L. W. Lau, A. R. Gerson and R. S. C. Smart, Resolving surface chemical states in XPS analysis of first row transition metals, oxides and hydroxides: Cr, Mn, Fe, Co and Ni, *Appl. Surf. Sci.*, 2011, **257**(7), 2717, DOI: **10.1016/j.apsusc.2010.10.051**.

29 E. Stavitski and F. M. De Groot, The CTM4XAS program for EELS and XAS spectral shape analysis of transition metal L edges, *Micron*, 2010, **41**(7), 687–694, DOI: **10.1016/j.micron.2010.06.005**.

30 F. M. de Groot, J. Fuggle, B. Thole and G. Sawatzky, 2p x-ray absorption of 3d transition-metal compounds: An atomic multiplet description including the crystal field, *Phys. Rev. B*, 1990, **42**(9), 5459, DOI: **10.1103/PhysRevB.42.5459**.

31 F. De Groot, Multiplet effects in X-ray spectroscopy, *Coord. Chem. Rev.*, 2005, **249**(1–2), 31–63, DOI: **10.1016/j.ccr.2004.03.018**.

32 A. Bocquet, T. Mizokawa, K. Morikawa, A. Fujimori, S. Barman, K. Maiti, D. Sarma, Y. Tokura and M. Onoda, Electronic structure of early 3d-transition-metal oxides by analysis of the 2p core-level photoemission spectra, *Phys. Rev. B*, 1996, **53**(3), 1161, DOI: **10.1103/PhysRevB.53.1161**.

33 J. Yeh and I. Lindau, Atomic subshell photoionization cross sections and asymmetry parameters: 1 Z 103, *At. Data Nucl. Data Tables*, 1985, **32**(1), 1–155, DOI: **10.1016/0092-640X(85)90016-6**.

34 E. L. Bullock, R. Gunnella, N. C. R. H. W. Yeom, S. Kono, R. I. G. Patthey, L. Johansson and C. R. Natoli, Angle dependence of the spin-orbit branching ratio, *Surf. Sci.*, 1996, **352–354**, 352, DOI: **10.1016/0039-6028(95)01159-5**.

35 N. I. of Standards, Technology, NIST Atomic Spectra Database, vol. **http://physics.nist.gov/asd3**, 2005.

36 N. Iordanova, M. Dupuis and K. M. Rosso, Theoretical characterization of charge transport in chromia, *J. Chem. Phys.*, 2005, **123**, 074710, DOI: **10.1063/1.2007607**.

37 M. C. Biesinger, C. Brown, J. R. Mycroft, N. S. Davidson and R. D. Mc Intyre, x-ray photoelectron spectroscopy of chromium compounfds, *Surf. Interface Anal.*, 2004, **36**(7), 1550, DOI: **10.1002/sia.1983**.

38 D. Briggs and P. Seah, Practical Surface Analysis,: *Auger and X-ray photoelectron spectroscopy*, Wiley, 1996, vol. 1.

39 L. Vattuone, A. Gerbi, D. Cappelletti, F. Pirani, R. Gunnella, L. Savio and M. Rocca, Selective Production of Reactive and Nonreactive Oxygen Atoms on Pd(001) by Rotationally Aligned Oxygen Molecules, *Angew. Chem., Int. Ed.*, 2009, **48**(26), 4845–4848, DOI: **10.1002/anie.200900870**.

40 R. Gunnella, P. Castrucci, N. Pinto, I. Davoli, D. Sebilleau and M. DeCrescenzi, X-ray photoelectron-diffraction study of intermixing and morphology at the Ge/Si(001) and Ge/Sb/Si(001) interface, *Phys. Rev. B*, 1996, **54**(12), 8882–8891, DOI: **10.1103/PhysRevB.54.8882**.

41 A. I. Poteryaev, M. Ferrero, A. Georges and O. Parcollet, Effect of crystal-field splitting and interband hybridization on the metal-insulator transitions of strongly correlated systems, *Phys. Rev. B*, 2008, **78**(4), 045115, DOI: **10.1103/PhysRevB.78.045115**.

42 R. Cheng, C. Borca, N. Pilet, B. Xu, L. Yuan, B. Doudin, S. H. Liou and P. A. Dowben, Oxidation of metals at the chromium oxide interface, *Appl. Phys. Lett.*, 2002, **81**(11), 2109–2111, DOI: **10.1063/1.1506942**.

